Protective Effects of Rutin Against Deltamethrin-Induced Hepatotoxicity and Nephrotoxicity in Rats via Regulation of Oxidative Stress, Inflammation and Apoptosis

Sefa Küçükler
Ataturk University: Ataturk Universitesi
Fatih Mehmet Kandemir
Ataturk University: Ataturk Universitesi
Selçuk Özdemir
Ataturk University: Ataturk Universitesi
Selim Çomaklı
Ataturk University: Ataturk Universitesi
Cuneyt Caglayan (ccaglayan@bingol.edu.tr)
Bingol Universitesi https://orcid.org/0000-0001-5608-554X

Research Article

Keywords: Apoptosis, Deltamethrin, Hepatotoxicity, Nephrotoxicity, Oxidative stress, Rutin

Posted Date: April 19th, 2021

DOI: https://doi.org/10.21203/rs.3.rs-392087/v1

Version of Record: A version of this preprint was published at Environmental Science and Pollution Research on July 3rd, 2021. See the published version at https://doi.org/10.1007/s11356-021-15190-w.

Abstract

Deltamethrin (DLM) is a type-II pyrethroid synthetic insecticide that is extensively used for controlling mosquitoes, flies, pests, insects worldwide. Oxidative stress is one of the DLM toxicity mechanisms. This study was carried out to evaluate the likelihood protective effects of rutin (RUT), a natural antioxidant, against DLM-induced liver and kidney toxicities in rats. Hepatotoxicity and nephrotoxicity were evaluated after the rats were treated orally with DLM (1.28 mg/kg b.w.) alone or with RUT (25 and 50 mg/kg b.w.) for 30 days. DLM administration caused an increase in lipid peroxidation level and a decrease in activities of SOD, CAT, and GPx and GSH levels in the both tissues. DLM also increased serum ALT, AST, ALP, urea, and creatinine levels, while reduced nephrine levels in rats. In addition, DLM increased the activation of inflammatory and apoptotic pathways by decreasing Bcl-2 and increasing TNF-α, NF-κB, IL-1β, p38α MAPK, COX-2, iNOS, beclin-1, Bax, and caspase-3 protein levels and/or activities. Furthermore, DLM increased mRNA expression levels of PARP-1, VEGF and immunohistochemical expressions of c-fos in the tissues. RUT treatment significantly improved all examined parameters and restored the liver and kidney histopathological and immunohistochemical alterations. These findings demonstrate that RUT could be used to ameliorate hepatotoxicity and nephrotoxicity associated with oxidative stress, inflammation, and apoptosis in DLM-induced rats.

1. Introduction

Exposure to environmental pollutants such as pesticides, xenobiotics, heavy metals and radiation has deleterious effects on human health and causes serious pathophysiological disorders. In particular, the rate of pesticides usage (including insecticides) due to their broad-spectrum bioactivity and low prices is alarming in countries where the main source of the economy is agriculture (Arora et al. 2016). Humans are potentially exposed to pesticides either directly, as farmers and agricultural workers, or indirectly, through the ingestion of contaminated food (Abdel-Daim &El-Ghoneimy 2015). Therefore, the intense use of pesticides can cause severe ecological threats and likelihood health issues, such as acute, subacute and chronic human and animal poisoning (Maalej et al. 2017).

Among pesticides, pyrethroid insecticides are one the most important classes of insecticides worldwide and account for more than 17% of the global agrochemical market (Li et al. 2017, Morgan et al. 2018). Deltamethrin (DLM) is a broad-spectrum type II synthetic pyrethroid insecticide, widely used to protect agricultural crops, fruits and vegetables against pests including as beetles, mites, ants and weevils (Abdel-Daim et al. 2013, Caglayan et al. 2020, Caglayan et al. 2019c). Accumulating evidence demonstrated that DLM is readily absorbed through contaminated food and water (Ahmadvand et al. 2016, Barlow et al. 2001). Despite its rapid metabolism and low toxicity, recent studies have shown that chronic exposure to DLM can cause adverse effects such as hepatotoxicity (Maalej et al. 2017), nephrotoxicity (Abdel-Daim &El-Ghoneimy 2015), neurotoxicity (Khalatbary et al. 2015), infertility (Abdallah et al. 2010) and metabolic disorders (Rjeibi et al. 2016). The accumulation of DLM particularly in liver and kidney tissues increases the generation of the reactive oxygen species (ROS). Increased ROS damages proteins, nucleic acids and lipids (Ahmadvand et al. 2016, Maalej et al. 2017). Therefore, the

investigation of the ways of protecting organs such as liver and kidney from such intoxication has attracted the attention of many researchers. It appears that natural antioxidants that can reduce tissue damage caused by DLM could be used for this purpose.

Rutin (RUT) is a flavonoid glycoside found in fruits and fruit peels, predominantly in citrus fruits such as grapefruit, oranges and lemons. It is also present in spinach, onions, apples, buckwheat seeds, tea, and wine (Çelik et al. 2020, Nafees et al. 2015). It has several pharmacological properties such as anti-inflammatory, antioxidant, antihypertensive, antiulcer, antiallergic, anti-carcinogenic, anti-mutagenic, immunomodulator and potent scavenger of superoxide radicals (Caglayan et al. 2019b, Kandemir et al. 2020a, Nafees et al. 2015). RUT has been documented to alleviate liver and/or kidney injuries induced by various toxic agents, including mercuric chloride (Caglayan et al. 2019a, Caglayan et al. 2019b), lead acetate (Ansar et al. 2016), carbon tetrachloride (Hafez et al. 2015), potassium bromate (Khan et al. 2012), acrylamide (Ahmed &Ibrahim Laila 2018) and hexachlorobutadiene (Sadeghnia et al. 2013).

Keeping in view the protective effects of RUT, the present study was designed to investigate the probable protective effects of RUT against DLM-induced hepatotoxicity and nephrotoxicity in male rats.

2. Materials And Methods

2.1. Chemicals

DLM ($C_{22}H_{19}Br_2NO_3$) is a synthetic pyrethroid insecticide (CAS Number: 52918-63-5, 98% purity). The CAS chemical name (α-cyano-3-phenoxybenzyl (1R,3R)-3-(2,2-dibromovinyl)-2,2 dimethyl cyclopropane carboxylate). RUT (3,3',4',5,7-pentahydroxyflavone-3-rhamnoglucoside, CAS Number: 207671-50-9, 94% purity) and other chemicals used in the study were supplied by Sigma–Aldrich Chemical Company (St. Louis, MO, USA).

2.2. Animals

Ten-week-old male Sprague Dawley rats (average body weight 250–300 g) were obtained from the Experimental Animal Center of Ataturk University, Erzurum, Turkey. The animal room was designed to maintain temperature at 24 ± 1°C, relative humidity at approximately 45 ± 5%, and a 12 h dark/light photoperiod. The rats were acclimatized to the experimental condition for a period of 1 week and fed with standard laboratory feed and tap water *ad-libitum.* The study was approved by the Animal Experiments Local Ethics Committee of the Atatürk University (Approval No: 2020-4 / 65).

2.3. Experimental design

The animals were randomly subdivided into 5 different groups with 7 rats in each group and were treated as follows:

Group I (Control) received 0.5 ml distilled water per rat, which was given only once a day via oral gavage.

Group II (RUT) received RUT (50 mg/kg, b. w.) (Manzoni et al. 2019).

Group III (DLM) received DLM (1.28 mg/kg, b. w.) (Yousef et al. 2006).

Group IV (DLM + RUT 25 mg/kg) was treated with rutin (25 mg/kg, b. w.) 30 min after DLM administration.

Group IV (DLM + RUT 50 mg/kg) was treated with RUT (50 mg/kg, b. w.) 30 min after DLM administration.

In present study, DLM and RUT were given orally through stomach gavage and continued for 30 consecutive days. DLM was dissolved in the distilled water and treated as it could completely dissolve and rapidly absorbed in the gastrointestinal tract (Kim et al. 2007). The selected dose of DLM was based on the previous study where 1/100 of the LD_{50} induced biochemical and histopathological alterations in rats without leading to morbidity (Yousef et al. 2006).

At the end of the experimental period, 24 h after receiving the last treatment, the rats were sacrificed under mild sevoflurane anesthesia. Blood samples were collected and centrifuged at 3000 rpm for 10 min to separate the serum. The liver and kidney tissues were used for biochemical, molecular and histopathological analysis.

2.4. Determination of hepatic and renal function markers

Measurement of serum levels of alanine aminotransferase (ALT), aspartate aminotransferase (AST) and alkaline phosphatase (ALP) were done by enzymatic commercial kits (TML, Diagnostic Medical Products, Ankara, Turkey). Also, serum levels of urea, creatinine and nephrin were measured by colorimetric kits (Diasis Diagnostic Systems, İstanbul, Turkey).

2.5. Determination of lipid peroxidation and antioxidant enzymes in the liver and kidney tissues

To obtain tissue homogenates, the liver and kidney tissues were ground using liquid nitrogen.

These tissues were homogenized in a homogenizer device with 1.15% potassium chloride to obtain a 1:10 (w/v) whole homogenate. The homogenates required for oxidative stress biomarkers and lipid peroxidation analyzes were obtained as described in our previous study (Kandemir et al. 2020b). Superoxide dismutase (SOD) activity of the liver and kidney tissue homogenates were estimated according to the method of Sun et al. (1988), and it was expressed as units (U)/g of protein. Catalase (CAT) activity was evaluated according to Aebi (1984), and it was expressed as katal/g of protein. Glutathione peroxidase (GPx) activity was evaluated as U/g protein in the liver and kidney tissues according to Lawrence andBurk (1976) method. Glutathione (GSH) content was determined by the method of Sedlak andLindsay (1968). As a marker of lipid peroxidation, the kidney and liver tissue malondialdehyde (MDA) concentrations were determined according to the method of Placer et al. (1966) and its levels were expressed as nmol/g of tissue. The GSH and MDA concentrations have been

expressed as nmol/g tissue. The protein content of the liver and kidney tissue homogenates were determined using the Lowry et al. (1951).

2.6. Determination of inflammatory markers in the liver and kidney tissues

Frozen liver and kidney tissues were homogenized in ice-cold phosphate saline buffer (0.1 M; pH 7.4; 1:20 w/v) and then centrifuged at 3500 rpm for 15 min to obtain these tissue homogenates. The obtained supernatants were used in the ELISA assays. Interleukin-1 beta (IL-1β), nuclear factor kappa B (NF-κB) and tumor necrosis factor-α (TNF-α) levels and p38α mitogen-activated protein kinase (p38α MAPK), inducible nitric oxide synthase (iNOS) and cyclooxygenase-2 (COX-2) activities in liver and kidney tissues were determined using commercial rat ELISA kits according to the manufacturer's procedure (YL Biont, Shanghai, China).

2.7. Determination of beclin-1 levels in the liver and kidney tissues

The levels of beclin-1 in the liver and kidney homogenates were determined using an ELISA kit according to the manufacturer's instructions (YL Biont, Shanghai, China).

2.8. Real Time PCR

Total RNA was isolated from liver and kidney tissue of experimental and control groups with QIAzol Lysis Reagent (Qiagen, Cat: 79306,Germany) according to the manufacturer’s instructions. cDNA was sythesized with QuantiTect Reverse Transcription (Qiagen, Cat:330411, Germany) from total RNA according to the manufacturer’s instructions (Özdemir &Çomaklı 2018). Real-time PCR (RT-PCR) was conducted to measure the mRNA transcript level of *Cas-3, Bax, Bcl-2, PARP-1*, and *VEGF* in the liver and kidney tissues using Rotor-Gene Q 5plex HRM Platform (Qiagen, Germany). All primer sequences and reaction conditions were shown in Table 1. GAPDH was used as internal control gene. Relative folds of expressions were evaluated with the $2^{-\Delta\Delta CT}$ method (Livak &Schmittgen 2001).

Table 1
Primer sequences of Cas-3, Bax, Bcl-2, PARP-1, VEGF, and GAPDH

Gene	Sequences (5'-3')	Length (bp)	Accession no
Cas-3	F: GGAGCTTGGAACGCGAAGAA R: ACACAAGCCCATTTCAGGGT	169	NM_012922.2
Bax	F: ACACCTGAGCTGACCTTGGA R: AGTTCATCGCCAATTCGCCT	115	NM_016993.1
Bcl-2	F: CTGGTGGACAACATCGCTCT R: GCATGCTGGGGCCATATAGT	115	NM_016993.1
PARP1	F: AAGGCGGAGAAGACATTGGG R: CGCATCTGGCCCTTCTCTAT	101	NM_007415.3
VEGF	F: AACTTCTGGGCTCTTCTCGC R: CTGGGACCACTTGGCATGGT	443	NM_001317041.1
GAPDH	F: AGTGCCAGCCTCGTCTCATA R: GATGGTGATGGGTTTCCCGT	248	NM_017008.4

2.9. Western Blot Analysis

Total protein was isolated from liver and kidney with Radioimmunoprecipitation assay buffer (RIPA buffer) and the protein concentration was measured by Bradford assay. Total proteins were separated by sodium dodecyl sulfate polyacrylamide gel electrophoresis (SDS/PAGE) on a 12% gel and transferred to a PDVF membrane. The membrane was incubated with primary antibodies; PARP (1:1000 dilution, Rabbit, ab227244, Abcam), VEGF (1:1000 dilution, Rabbit Polyclonal, ab46154, Abcam), and GAPDH (1:2000 dilution, Rabbit Polyclonal, ab9485, Abcam) overnight at 4°C on a shaker. The membrane was incubated with the secondary antibodies (goat anti-rabbit IgG-HRP 1:5000 dilution, ab6721, Abcam) at room temperature (RT) for 1 h. The target protein bands were analyzed using the ChemiDoc™ MP Imaging System (Bio-Rad, California, USA).

2.10. Histopathological processing

Liver and kidney tissues were first fixed in 10% neutral buffered formalin for 24 h and then were washed with tap water. Tissues were processed for dehydration with a series of graded ethanol (70, 80, 90, 96, 100%) and xylene series and embedded in paraffin. 5 µm thick were obtained with a microtome (Leica RM2255, Germany). Later, sections were deparaffinised, rehydrated and stained with the hematoxylin-eosin solution for observation for pathological damage.

2.11. Immunohistochemistry

Immunohistochemical detection of c-fos was performed using the streptavidin-biotin peroxidase technique. Serial sections of 5 µm thickness were placed on poly-l-lysine coated slides, deparaffinized, dehydrated, rinsed in tap water, and treated with 3 % H_2O_2 to quench the endogenous peroxidase activity for 10 min, then immersed in heated sodium citrate buffer (10 mM, pH 6.0) for 20 min, then cooled for 20 min. The slides were incubated in a blocking solution to block nonspecific protein bindings for 10 min at room temperature. The slides were then incubated with the primary antibody (c-fos; Cat no: sc-166940, Santa Cruz Biotechnology) diluted 1:100 for 1 h at room temperature. Thereafter, the sections were incubated with the appropriate biotin, then streptavidin peroxidase (UltraVision™ Large Volume Detection System, Thermo Scientific/Lab Vision, TP-125-HL) at room temperature, 15 min for each. The primary-seconder antibody complex was visualized using 3, 3'diaminobenzidine (DAB) chromogen, then tissues were counterstained with Mayer's hematoxylin, dehydrated, cleared and mounted with coverslips. The immunohistochemistry results were evaluated semi-quantitatively as follows: none = -; mild = +; moderate = ++; intense = +++.

2.12. Statistical analysis

IBM SPSS 20 was used to perform statistical analyses. One-Way Analysis of Variance (ANOVA) used to detect statistically differences of *Cas-3, Bax, Bcl-2, PARP-1, and VEGF* expressions at mRNA level between control and treatment groups. RT-PCR results are expressed as mean ± SEM. Statistically differences were considered to be significant at $p < 0.05$, $p < 0.01$ and $p < 0.001$.

The immunohistochemistry data were analyzed using SPSS software and compared by one-way analysis of variance followed by Tukey’s test. Data are means ± standard errors of the mean (SEM). $p < 0.05$ was regarded as statistically significant.

3. Results

3.1. RUT prevents DLM-induced liver injury

Oral administration of DLM caused a significant elevation ($p < 0.05$) of serum ALT, AST and ALP activities compared to the control group. Concurrent administration of RUT (25 and 50 mg/kg) significantly alleviated ($p < 0.05$) serum AST, ALP and ALT activities in DLM-induced rats (Table 2).

Table 2
Protective effect of rutin on liver serum markers and oxidative stress biomarkers in DLM-induced hepatotoxicity

Parameters	Control	RUT	DLM	DLM + RUT25	DLM + RUT50
ALP (U/L)	74.99 ± 1.95[a]	76.06 ± 1.92[a]	220.72 ± 6.42[c]	121.25 ± 4.59[b]	108.82 ± 4.46[b]
ALT (U/L)	43.97 ± 0.73[a]	44.69 ± 0.53[a]	93.14 ± 0.88[d]	73.72 ± 1.38[c]	55.61 ± 0.90[b]
AST (U/L)	53.92 ± 1.13[a]	54.13 ± 0.84[a]	92.95 ± 1.60[d]	78.12 ± 1.17[c]	63.38 ± 0.75[b]
MDA (nmol/g tissue)	39.98 ± 0.59[a]	40.31 ± 0.70[a]	61.84 ± 0.94[d]	53.71 ± 0.79[c]	48.04 ± 0.66[b]
GSH (nmol/g tissue)	6.17 ± 0.07[d]	6.14 ± 0.15[d]	2.99 ± 0.09[a]	4.00 ± 0.07[b]	5.08 ± 0.09[c]
SOD (U/g tissue)	46.43 ± 0.75[d]	45.92 ± 0.63[d]	25.46 ± 0.52[a]	30.93 ± 0.61[b]	39.59 ± 0.83[c]
CAT (katal/g protein)	59.94 ± 0.70[c]	60.13 ± 0.58[c]	39.72 ± 0.59[a]	49.82 ± 1.46[b]	52.12 ± 0.94[b]
GPx (U/g tissue)	46.23 ± 0.49[d]	47.62 ± 0.65[d]	22.15 ± 0.82[a]	33.80 ± 0.73[b]	39.49 ± 0.93[c]

Different superscripts (a–d) in the same row indicate significant difference ($p < 0.05$) among groups.

3.2. RUT protects DLM-induced kidney injury

The effects of RUT treatment on the DLM-induced kidney toxicity on serum urea, creatinine and nephrin levels are shown in Table 3. Treatment with DLM resulted in a highly significant increase in serum urea and creatinine levels ($p < 0.05$) and a significant decrease in serum nephrin level ($p < 0.05$) as compared to the control groups while co-treatment of RUT caused a significant decline in the levels of serum urea and creatinine, and a significant increase in the level of nephrin.

Table 3
Protective effect of rutin on kidney serum markers and oxidative stress biomarkers in DLM-induced nephrotoxicity

Parameters	Control	RUT	DLM	DLM + RUT25	DLM + RUT50
Nephrin (mg/dL)	39.09 ± 0.57[d]	39.39 ± 0.67[d]	24.38 ± 0.49[a]	29.44 ± 0.66[b]	34.16 ± 0.54[c]
Urea (mg/dL)	29.58 ± 0.80[a]	27.62 ± 0.51[a]	50.65 ± 0.75[d]	42.87 ± 0.65[c]	36.79 ± 0.60[b]
Creatinine (mg/dL)	0.45 ± 0.01[a]	0.45 ± 0.01[a]	1.87 ± 0.03[d]	1.34 ± 0.03[c]	0.62 ± 0.03[b]
MDA (nmol/g tissue)	35.91 ± 0.62[a]	35.86 ± 0.63[a]	57.07 ± 0.67[d]	47.65 ± 0.67[c]	41.71 ± 0.72[b]
GSH (nmol/g tissue)	4.44 ± 0.06[d]	4.53 ± 0.06[d]	2.38 ± 0.07[a]	3.28 ± 0.04[b]	3.91 ± 0.06[c]
SOD (U/g tissue)	34.95 ± 0.56[d]	35.45 ± 0.72[d]	16.91 ± 0.57[a]	24.79 ± 0.28[b]	28.95 ± 0.59[c]
CAT (katal/g protein)	40.21 ± 0.52[c]	40.96 ± 0.61[c]	22.39 ± 0.70[a]	32.45 ± 0.59[b]	34.74 ± 0.60[b]
GPx (U/g tissue)	38.17 ± 0.65[d]	39.25 ± 0.68[d]	24.73 ± 0.30[a]	32.45 ± 0.59[b]	34.74 ± 0.60[c]

Different superscripts (a–d) in the same row indicate significant difference ($p < 0.05$) among groups.

3.3. Effect of RUT and DLM on liver and kidney oxidative stress markers

To research the roles of antioxidant enzymes in mediating the radical-scavenging activity of RUT, the lipid peroxidation and intracellular antioxidant enzyme activities were measured in the DLM-induced hepatotoxicity and nephrotoxicity. It was observed that the MDA levels in liver and kidney tissues of rats treated with DLM alone caused a significant increase ($p < 0.05$) compared to the control group. This increase was attenuated by the treatment with RUT. Additionally, significantly reduced activities of the enzymatic (SOD, CAT, and GPx) and non-enzymatic (GSH) antioxidant molecules were seen in the liver and kidney tissues of DLM-treated rats compared with the control group. Co-administration of RUT (25 and 50 mg/kg) with DLM significantly increased the above-mentioned parameters in a dose-dependent manner compared to the DLM group alone.

3.4. Effect of RUT and DLM on liver and kidney inflammatory markers

To explore the effects of RUT treatment on the inflammatory response with DLM administration, we determined liver and kidney NF-κB, TNF-α, IL-1β, iNOS and COX-2 levels. DLM-induced groups showed a significant increase ($p < 0.05$) in liver and kidney NF-κB, TNF-α and IL-1β levels when compared with the control groups as depicted in Fig. 1A-C. However, concurrent administration of RUT led to a significant decrease ($p < 0.05$) in these levels in DLM-induced groups.

Activities of iNOS and COX-2 showed a significant ($p < 0.05$) increase in the liver and kidney tissues of DLM-induced rats when compared to the control group (Fig. 2A and 2B). The combination of DLM and RUT downregulated ($p < 0.05$) the high levels of these enzymes compared to the DLM-induced group.

3.5. Effect of RUT and DLM on liver and kidney p38α MAPK and beclin-1 levels

The levels of p38α MAPK and beclin-1 in liver and kidney tissues were studied by rat ELISA kits. The results showed that the levels of p38α MAPK and beclin-1 in these tissues increased significantly after DLM treatment compared to the control group while both doses of RUT significantly ($p < 0.05$) decreased p38α MAPK and beclin-1 levels compared to DLM group.

3.6. RUT decreased the apoptosis activity induced by DLM

While *Cas-3* and *Bax* mRNA transcipt level was up-regulated in the DLM group compared to control ($p < 0.01$), these genes expression was down-regulated in the the DLM + RUT 25 and DLM + RUT 50 groups compared to the DLM group ($p < 0.05$). Furthermore, Bcl-2 mRNA transcipt level was down regulated in the DLM group compared to control ($p < 0.01$). However, Bcl-2 gene expression was up-regulated in the the DLM + RUT 25 and DLM + RUT 50 groups compared to the DLM group ($p < 0.05$) (Figs. 3A-3C). These results indicated that while DLM treatment induced the apoptosis in the liver and kidney tissues, RUT decreased the apoptosis.

3.7. RUT reduced the expressions of PARP-1 and VEGF induced by DLM

PARP-1 and *VEGF* gene expression levels were only up-regulated in the DLM group compared to the control group ($p < 0.01$). In the RUT group, the mRNA transcript levels of *PARP-1* and *VEGF* were similar as the control group for both liver and kidney tissue ($p > 0.05$). *PARP-1* and *VEGF* gene expression levels were down-regulated in the DLM + RUT25 and DLM + RUT 50 groups compared to the DLM group ($p < 0.05$) (Figs. 4A-4B). In addition, the Western Blot results of PARP-1 and VEGF confirmed the RT-PCR results. While, the protein levels of PARP-1 and VEGF were increased in the DLM group, these protein levels were decreased in the DLM + RUT 25 and DLM + RUT 50 ($p < 0.05$) (Figs. 4C-4D). These results indicated that while DLM treatment activated the PARP-1 and VEGF in the liver and kidney tissues of rats, RUT deactivated the these gene expressions.

3.8. Effect of RUT treatment on the histopathology of DLM treated rats

Normal hepatocytes with normal sinusoids and the central vein were seen both in control rats (Fig. 5A) and only RUT-treated rats (Fig. 5B). DLM caused extremely severe hemorrhage, necrosis, and dissociation in hepatocytes around the central vein in rats as shown in Fig. 5C. In the DLM + RUT 25-treated group showed severe congestion, moderate necrosis (Fig. 5D). RUT50 treatment significantly alleviated DLM induced increase in congestion and necrosis (Fig. 5E).

There were not seen any pathological findings within the corticomedullary junction in the control (Fig. 6A) and only RUT-treated groups (Fig. 6B). Histopathological findings showed severe necrosis and hemorrhage in the corticomedullary junction in the DLM-treated groups (Fig. 6C). In contrast, treatment with RUT 25 demonstrated a mild reduction of the hemorrhage in the corticomedullary junction (Fig. 6D). Treatment of DLM + RUT50 also provided a more significant reduction in hemorrhage (Fig. 6E).

3.9. Effect of RUT on the expression of c-fos in DLM-treated rats

Immunohistochemical staining of c-fos in rat liver showed no c-fos expression in the control (Fig. 7A) and RUT-treated groups (Fig. 7B) with a significant increase in c-fos expression in the cytoplasm of hepatocytes in the DLM-treated group (Fig. 7C); a significant decrease in c-fos expression in the groups treated with DLM + RUT 50 group (Fig. 7E), while the DLM + RUT 25 group showed no a significant decrease c-fos expression (Fig. 7D; Table 4, $p < 0.05$). Immunohistochemical staining of c-fos in rats kidney showed no expression in the cytoplasm of tubular epithelium in the corticomedullar junction of the control (Fig. 8A) and RUT-treated groups (Fig. 8B). A significant increase in c-fos expression was recorded in the DLM-treated group (Fig. 8C) as compared to the control group and RUT-treated group. A significant decrease was recorded in c-fos expression in the DLM + RUT 25 (Fig. 8D) and DLM + RUT 50 treated group (Fig. 8E) and showed a significant change as compared to the control group (Table 4, $p < 0.05$).

Table 4
Effect of rutin on c-fos expression in DLM-induced liver and kidney damage in rats

Organs	Control	RUT	DLM	DLM + RUT25	DLM + RUT25
Liver	0.28 ± 0.18	0.42 ± 0.29	2.57 ± 0.29*	2.57 ± 0.20*	1.42 ± 0.20#
Kidney	0.28 ± 0.18	0.14 ± 0.14	2.57 ± 0.20*	1.57 ± 0.29#	1.28 ± 0.28#
Values are shown as mean ± SEM.					
*significant difference as compared to the mean value observed in control and rutin groups ($p < 0.05$).					
#significant difference as compared to the mean value observed in DLM group ($p < 0.05$)					

4. Discussion

Although pyrethroid insecticides were initially thought not to be hazardous to human and mammalian health, further investigations of synthetic pyrethroids have been shown to have possible toxic effects.

Free radicals and ROS may play crucial roles in the induction of pyrethroids-induced damage to proteins, lipids and DNA in both invertebrates and vertebrates. Among the pyrethroid insecticides, DLM has been reported to have some toxic effects (El Golli-Bennour et al. 2019, Maalej et al. 2017). Liver microsomal enzymes which mainly metabolize DLM and toxic metabolites of DLM have been documented to accumulate in the liver (Abdelkhalek et al. 2015, El Golli-Bennour et al. 2019). Toxic metabolites of DLM mainly accumulates in liver as it is the main site of metabolism of xenobiotics and the kidney is the main excretory organ (Abdelkhalek et al. 2015, Sayeed et al. 2003). A group of scientists have shown that DLM can easily penetrate the membrane cell due to its lipophilic nature and cause lipid peroxidation (Abdel-Daim et al. 2013). Based on the previous studies, it has been emphasized that one of the main causes of hepatotoxicity and nephrotoxicity caused by DLM is oxidative stress (Abdel-Daim &El-Ghoneimy 2015, Rjeibi et al. 2016). Present study demonstrared that DLM administration was associated with a significant increase in MDA level (as a marker of lipid peroxidation) as well as by a decrease in the activity of SOD, CAT, GPx and GSH in both tissues (Tables 2 and 3). However, administration of RUT reduced DLM-induced liver and kidney damages by increasing antioxidant enzyme activities that had been reduced by DLM. In a similiar study, it was found that RUT ameliorated reduced antioxidant enzyme activities in carbon tetrachloride-induced hepatotoxicity and nephrotoxicity in rats (Elsawy et al. 2019).

Liver biomarker enzymes such as ALP, ALT and AST are used as markers of liver damage, while urea, creatinine, and nephrine are considered markers of kidney function and in some recent studies, a notable elevation of levels of these biomarkers was observed after DLM intoxication (Abdel-Daim &El-Ghoneimy 2015, Maalej et al. 2017). The histopathologic observation of liver tissue in DLM-treated rats showed severe hemorrhage, necrosis, and dissociation in hepatocytes around the central vein. Also, severe necrosis and hemorrhage in the corticomedullary junction have been observed in the DLM-treated rat kidney tissues. In the present study, co-treatment with RUT significantly ameliorated DLM-induced liver and kidney injuries and decreased elevations of above-mentioned serum biomarker levels. These results revealed the antioxidant effect of RUT, which plays an important role in reducing toxicity and maintaining liver and kidney membrane integrity in DLM-treated rats.

ROS can activate several transcription factors, which causes to the differential expression of some genes participated in inflammatory pathways (Hussain et al. 2016). Under different pathological conditions, the classical NF-κB inflammatory signaling pathway is activated by ROS. Following that, many pro-inflammatory cytokines such as TNF-α, IL-1β, IL-6, COX-2, and iNOS are released and this further exacerbates the inflammatory injury to the liver and kidney (Kandemir et al. 2019, Li et al., Temel et al. 2020). Previously, it has been shown that DLM exposure increased the expression of inflammatory markers such as NFκB, TNFα, COX-2, and iNOS in rats' primary hepatocytes (Arora et al. 2016). However, the mechanism by which DLM induces inflammation remains unclear. In our study, we showed that RUT plays an important role in alleviating ROS generated and NFκB induced inflammation through reduction of TNF-α, IL-1β, p38α-MAPK, COX-2 and iNOS in the liver and kidney damages caused by DLM. In our previous studies, we reported that the combination of RUT with mercury chloride reduced liver and kidney inflammation by reducing the levels of inflammation-related parameters (Caglayan et al. 2019a, Caglayan et al. 2019b).

Apoptosis is a normal cellular death-process triggered by some factors that include toxins (Ahmadvand et al. 2016). Previously, *in vivo* and *in vitro* studies demonstrated that exposure to DLM significantly affected cell survival and induced apoptosis in hepatocytes (Das et al. 2007), kidneys (Maalej et al. 2017), splenocytes (Kumar &Sharma 2015), neuronal cells (Wu et al. 2000), and PC12 cells (Park et al. 2017). Recent evidence has shown that DLM exposure may induce caspase independent/dependent death in a variety of cells/tissues (Arora et al. 2016, Kumar et al. 2016, Kumar &Sharma 2015, Park et al. 2017). It has also been reported that DLM can induce cell damage through activation of multiple pathways, including but not restricted to caspase activation; ER stress signaling; eNOS / JNK / AR pathways, calpain mediated cell death, altered intracellular calcium level or autophagic modulation. (Hossain &Richardson 2011, Kumar et al. 2016, Magby &Richardson 2015, Park et al. 2017, Yu et al. 2014). Maalej et al. (2017) have manifested that DLM induced apoptosis by increasing expression of p53 as well as decreasing bcl-2 in rat liver and kidney tissues. In the current study, we observed increased mRNA expression of apoptotic markers *Bax* and *caspase-3*, while *Bcl-2* expression was decreased in DLM-induced rat liver and kidney tissues. Conversely, co-treatment of RUT was significantly effective in reversing apoptosis in these tissues.

VEGF is an endothelial cell mitogen that is mainly synthesized due to tissue ischemia, hypoxia and endothelial cell damage (Atakan et al. 2008). It plays a role in wound healing, vascular permeabilization, inflammation, embryogenesis, and tissue remodeling (Neufeld et al. 1999, Shihab et al. 2003). It has been documented that VEGF plays an important role in angiogenesis, nephrogenesis and hepatic regeneration (Ferrara 1999, Papastefanou et al. 2007). PARP-1 is a nuclear protein involved in the routine repair of DNA damage by adding poly (ADP ribose) polymers in response to various cellular stresses (Chaitanya et al. 2010). During oxidative stress, PARP-1 acts as a DNA break resulting in transient ribosylation using endogenous NAD^+ as the ribose monomer substrate donor (Coyle et al. 2015). In addition, increased activation of PARP-1 can lead to cell death and organ damage as a result of depletion of cellular reducing equivalents (e.g., NADH) and cellular energy crisis (Hegedűs &Virág 2014). It has been reported that DNA damage associated with oxidative stress can induce PARP-1 activation (Hegedűs &Virág 2014, Virag 2005). RT-PCR and immunoblotting results in this study confirmed that DLM toxicity caused an increase in PARP-1 and VEGF expression in liver and kidney tissues, while RUT treatment significantly decreased the expression of these parameters compared to only DLM group.

C-fos is an important member of activator-protein 1 (AP-1) participated in cellular processes some of which include cell proliferation, differentiation and apoptotic cell death (Kadry et al. 2018, Stanisavljević et al. 2019). C-fos also was shown to function as a suppressor protein in inflammatory responses. It directly interacts directly p65 subunit of NF-κB, consequently inhibiting the pathway downstream of NF-κB and triggering of pro-inflammatory cytokines such as TNF-α (Ray et al. 2006). In the present study, we found a remarkable increase in the expression of c-fos in the liver and kidney tissues of rats in the DLM-induced group, and co-treatment with RUT reduced its overexpression.

Conclusions

This study concluded that DLM-induced hepatotoxicity and nephrotoxicity by promoting oxidative stress, inflammatory, and apoptotic mechanisms. Treatment with RUT significantly ameliorated all biochemical, molecular and histological changes, induced by DLM. Therefore, RUT is considered to be an effective hepatoprotective and nephroprotective agent, pending further detailed mechanistic studies.

Declarations

Author contribution

SK: investigation, methodology. FMK: investigation, data curation, review & editing, supervision, SÖ: methodology, software, formal analysis. SÇ: methodology, formal analysis. CC: investigation, writing - review & editing, supervision.

Funding

This work was not supported by any funding.

Data Availability

Not applicable

Ethics approval

The animal care and use procedures applied in the study were conducted under the protocols approved by the Animal Experiments Local Ethics Committee of the Atatürk University (Approval No: 2020-4 / 65).

Consent to participate

Not applicable

Consent for publication

Not applicable

Conflict of interest

The authors have declared no conflicts of interest.

References

1. Abdallah FB, Slima AB, Dammak I, Keskes-Ammar L, Mallek Z (2010): Comparative effects of dimethoate and deltamethrin on reproductive system in male mice. Andrologia 42, 182-186
2. Abdel-Daim MM, Abuzead SM, Halawa SM (2013): Protective role of Spirulina platensis against acute deltamethrin-induced toxicity in rats. PLoS One 8, e72991

3. Abdel-Daim MM, El-Ghoneimy A (2015): Synergistic protective effects of ceftriaxone and ascorbic acid against subacute deltamethrin-induced nephrotoxicity in rats. Ren. Fail. 37, 297-304
4. Abdelkhalek NK, Ghazy EW, Abdel-Daim MM (2015): Pharmacodynamic interaction of Spirulina platensis and deltamethrin in freshwater fish Nile tilapia, Oreochromis niloticus: impact on lipid peroxidation and oxidative stress. Environmental Science and Pollution Research 22, 3023-3031
5. Aebi H (1984): [13] Catalase in vitro, Methods in enzymology. Elsevier, pp. 121-126
6. Ahmadvand H, Ghabaee DNZ, Malekshah AK, Navazesh A (2016): Virgin olive oil ameliorates deltamethrin-induced nephrotoxicity in mice: A biochemical and immunohistochemical assessment. Toxicology Reports 3, 584-590
7. Ahmed MM, Ibrahim Laila IM (2018): Rutin Ameliorates Acrylamide-Induced Hepatotoxicity and Biochemical Disturbance in Male Albino Rats. Scientific Journal of October 6 University 4, 8-13
8. Ansar S, Hamed S, AlGhosoon H, AlSaedan R, Iqbal M (2016): The protective effect of rutin against renal toxicity induced by lead acetate. Toxin Rev. 35, 58-62
9. Arora D, Siddiqui MH, Sharma PK, Shukla Y (2016): Deltamethrin induced RIPK3-mediated caspase-independent non-apoptotic cell death in rat primary hepatocytes. BBRC 479, 217-223
10. Atakan A, Arikan H, Macunluoglu B, Tuglular S, Ulfer G, Cakalagaoglu F, Ozener C, Akoglu E (2008): Renal protective effects of leukotriene receptor blockers in an experimental model of cyclosporine nephrotoxicity, Transplantation proceedings. Elsevier, pp. 279-284
11. Barlow S, Sullivan F, Lines J (2001): Risk assessment of the use of deltamethrin on bednets for the prevention of malaria. Food Chem. Toxicol. 39, 407-422
12. Caglayan C, Kandemir FM, Darendelioğlu E, Yıldırım S, Kucukler S, Dortbudak MB (2019a): Rutin ameliorates mercuric chloride-induced hepatotoxicity in rats via interfering with oxidative stress, inflammation and apoptosis. J. Trace Elem. Med. Biol. 56, 60-68
13. Caglayan C, Kandemir FM, Yildirim S, Kucukler S, Eser G (2019b): Rutin protects mercuric chloride-induced nephrotoxicity via targeting of aquaporin 1 level, oxidative stress, apoptosis and inflammation in rats. J. Trace Elem. Med. Biol. 54, 69-78
14. Caglayan C, Taslimi P, Türk C, Kandemir FM, Demir Y, Gulcin İ (2019c): Purification and characterization of the carbonic anhydrase enzyme from horse mackerel (Trachurus trachurus) muscle and the impact of some metal ions and pesticides on enzyme activity. Comparative Biochemistry and Physiology Part C: Toxicology & Pharmacology 226, 108605
15. Caglayan C, Taslimi P, Türk C, Gulcin I, Kandemir FM, Demir Y, Beydemir Ş (2020): Inhibition effects of some pesticides and heavy metals on carbonic anhydrase enzyme activity purified from horse mackerel (Trachurus trachurus) gill tissues. Environmental Science and Pollution Research, 1-10
16. Chaitanya GV, Alexander JS, Babu PP (2010): PARP-1 cleavage fragments: signatures of cell-death proteases in neurodegeneration. Cell Communication and Signaling 8, 31
17. Coyle JP, Mayo-Perez A, Bourgeois M, Johnson G, Morris S, Harbison R (2015): The assessment of an in-vitro model for evaluating the role of PARP in ethanol-mediated hepatotoxicity. International Journal of Critical Illness and Injury Science 5, 9

18. Çelik H, Kandemir FM, Caglayan C, Özdemir S, Çomaklı S, Kucukler S, Yardım A (2020): Neuroprotective effect of rutin against colistin-induced oxidative stress, inflammation and apoptosis in rat brain associated with the CREB/BDNF expressions. Mol. Biol. Rep. 47, 2023-2034
19. Das PC, Streit TM, Cao Y, Rose RL, Cherrington N, Ross MK, Wallace AD, Hodgson E (2007): Pyrethroids: Cytotoxicity and Induction of CYP Isoforms Human Hepatocytes. Drug Metabolism & Drug Interactions (DMDI) 23, 211
20. El Golli-Bennour E, Timoumi R, Annaibi E, Mokni M, Omezzine A, Bacha H, Abid-Essefi S (2019): Protective effects of kefir against deltamethrin-induced hepatotoxicity in rats. Environmental Science and Pollution Research 26, 18856-18865
21. Elsawy H, Badr GM, Sedky A, Abdallah BM, Alzahrani AM, Abdel-Moneim AM (2019): Rutin ameliorates carbon tetrachloride (CCl4)-induced hepatorenal toxicity and hypogonadism in male rats. PeerJ 7, e7011
22. Ferrara N (1999): Role of vascular endothelial growth factor in the regulation of angiogenesis. Kidney Int. 56, 794-814
23. Hafez MM, Al-Harbi NO, Al-Hoshani AR, Al-Hosaini KA, Al Shrari SD, Al Rejaie SS, Sayed-Ahmed MM, Al-Shabanah OA (2015): Hepato-protective effect of rutin via IL-6/STAT3 pathway in CCl 4-induced hepatotoxicity in rats. Biol. Res. 48, 30
24. Hegedűs C, Virág L (2014): Inputs and outputs of poly (ADP-ribosyl) ation: Relevance to oxidative stress. Redox biology 2, 978-982
25. Hossain MM, Richardson JR (2011): Mechanism of pyrethroid pesticide–induced apoptosis: role of Calpain and the ER stress pathway. Toxicol. Sci. 122, 512-525
26. Hussain T, Tan B, Yin Y, Blachier F, Tossou MC, Rahu N (2016): Oxidative stress and inflammation: what polyphenols can do for us? Oxid. Med. Cell. Longev. 2016
27. Kadry MO, Abdel-Megeed RM, El-Meliegy E, Abdel-Hamid A-HZ (2018): Crosstalk between GSK-3, c-Fos, NFκB and TNF-α signaling pathways play an ambitious role in Chitosan Nanoparticles Cancer Therapy. Toxicology reports 5, 723-727
28. Kandemir FM, Yildirim S, Caglayan C, Kucukler S, Eser G (2019): Protective effects of zingerone on cisplatin-induced nephrotoxicity in female rats. Environmental Science and Pollution Research 26, 22562-22574
29. Kandemir FM, Caglayan C, Aksu EH, Yildirim S, Kucukler S, Gur C, Eser G (2020a): Protective effect of rutin on mercuric chloride-induced reproductive damage in male rats. Andrologia 52, e13524
30. Kandemir FM, Yıldırım S, Kucukler S, Caglayan C, Darendelioğlu E, Dortbudak MB (2020b): Protective effects of morin against acrylamide-induced hepatotoxicity and nephrotoxicity: A multi-biomarker approach. Food Chem. Toxicol. 138, 111190
31. Khalatbary AR, Ghaffari E, Mohammadnegad B (2015): Protective role of oleuropein against acute deltamethrin-induced neurotoxicity in rat brain. Iran Biomed J 19, 247
32. Khan RA, Khan MR, Sahreen S (2012): Protective effects of rutin against potassium bromate induced nephrotoxicity in rats. BMC Complement. Altern. Med. 12, 204

33. Kim K-B, Anand SS, Muralidhara S, Kim HJ, Bruckner JV (2007): Formulation-dependent toxicokinetics explains differences in the GI absorption, bioavailability and acute neurotoxicity of deltamethrin in rats. Toxicology 234, 194-202
34. Kumar A, Sharma N (2015): Comparative efficacy of piperine and curcumin in deltamethrin induced splenic apoptosis and altered immune functions. Pestic. Biochem. Physiol. 119, 16-27
35. Kumar A, Sasmal D, Bhaskar A, Mukhopadhyay K, Thakur A, Sharma N (2016): Deltamethrin-induced oxidative stress and mitochondrial caspase-dependent signaling pathways in murine splenocytes. EnTox 31, 808-819
36. Lawrence RA, Burk RF (1976): Glutathione peroxidase activity in selenium-deficient rat liver. BBRC 71, 952-958
37. Li H, Cheng F, Wei Y, Lydy MJ, You J (2017): Global occurrence of pyrethroid insecticides in sediment and the associated toxicological effects on benthic invertebrates: an overview. J. Hazard. Mater. 324, 258-271
38. Li S, Zheng X, Zhang X, Yu H, Han B, Lv Y, Liu Y, Wang X, Zhang Z Exploring the liver fibrosis induced by deltamethrin exposure in quails and elucidating the protective mechanism of resveratrol. Ecotoxicol. Environ. Saf. 207, 111501
39. Livak KJ, Schmittgen TD (2001): Analysis of relative gene expression data using real-time quantitative PCR and the 2− ΔΔCT method. Methods 25, 402-408
40. Lowry OH, Rosebrough NJ, Farr AL, Randall RJ (1951): Protein measurement with the Folin phenol reagent. J. Biol. Chem. 193, 265-275
41. Maalej A, Mahmoudi A, Bouallagui Z, Fki I, Marrekchi R, Sayadi S (2017): Olive phenolic compounds attenuate deltamethrin-induced liver and kidney toxicity through regulating oxidative stress, inflammation and apoptosis. Food Chem. Toxicol. 106, 455-465
42. Magby JP, Richardson JR (2015): Role of Calcium and Calpain in the Downregulation of Voltage-Gated Sodium Channel Expression by the Pyrethroid Pesticide Deltamethrin. J. Biochem. Mol. Toxicol. 29, 129-134
43. Manzoni AG, Passos DF, da Silva JL, Bernardes VM, Bremm JM, Jantsch MH, de Oliveira JS, Mann TR, de Andrade CM, Leal DB (2019): Rutin and curcumin reduce inflammation, triglyceride levels and ADA activity in serum and immune cells in a model of hyperlipidemia. Blood Cells Mol. Dis. 76, 13-21
44. Morgan MK, MacMillan DK, Zehr D, Sobus JR (2018): Pyrethroid insecticides and their environmental degradates in repeated duplicate-diet solid food samples of 50 adults. J. Expo. Sci. Environ. Epidemiol. 28, 40-45
45. Nafees S, Rashid S, Ali N, Hasan SK, Sultana S (2015): Rutin ameliorates cyclophosphamide induced oxidative stress and inflammation in Wistar rats: role of NFκB/MAPK pathway. Chem.-Biol. Interact. 231, 98-107
46. Neufeld G, Cohen T, Gengrinovitch S, Poltorak Z (1999): Vascular endothelial growth factor (VEGF) and its receptors. The FASEB journal 13, 9-22

47. Özdemir S, Çomaklı S (2018): Investigation of the interaction between bta-miR-222 and the estrogen receptor alpha gene in the bovine ovarium. Reprod. Biol. 18, 259-266
48. Papastefanou VP, Bozas E, Mykoniatis MG, Grypioti A, Garyfallidis S, Bartsocas CS, Nicolopoulou-Stamati P (2007): VEGF isoforms and receptors expression throughout acute acetaminophen-induced liver injury and regeneration. Arch. Toxicol. 81, 729-741
49. Park YS, Park JH, Ko J, Shin IC, Koh HC (2017): m TOR inhibition by rapamycin protects against deltamethrin-induced apoptosis in PC 12 Cells. EnTox 32, 109-121
50. Placer ZA, Cushman LL, Johnson BC (1966): Estimation of product of lipid peroxidation (malonyl dialdehyde) in biochemical systems. AnBio 16, 359-364
51. Ray N, Kuwahara M, Takada Y, Maruyama K, Kawaguchi T, Tsubone H, Ishikawa H, Matsuo K (2006): c-Fos suppresses systemic inflammatory response to endotoxin. Int. Immunol. 18, 671-677
52. Rjeibi I, Saad AB, Hfaiedh N (2016): Oxidative damage and hepatotoxicity associated with deltamethrin in rats: The protective effects of Amaranthus spinosus seed extract. Biomed. Pharmacother. 84, 853-860
53. Sadeghnia HR, Yousefsani BS, Rashidfar M, Boroushaki MT, Asadpour E, Ghorbani A (2013): Protective effect of rutin on hexachlorobutadiene-induced nephrotoxicity. Ren. Fail. 35, 1151-1155
54. Sayeed I, Parvez S, Pandey S, Bin-Hafeez B, Haque R, Raisuddin S (2003): Oxidative stress biomarkers of exposure to deltamethrin in freshwater fish, Channa punctatus Bloch. Ecotoxicol. Environ. Saf. 56, 295-301
55. Sedlak J, Lindsay RH (1968): Estimation of total, protein-bound, and nonprotein sulfhydryl groups in tissue with Ellman's reagent. AnBio 25, 192-205
56. Shihab FS, Bennett WM, Isaac J, Yi H, Andoh TF (2003): Nitric oxide modulates vascular endothelial growth factor and receptors in chronic cyclosporine nephrotoxicity. Kidney Int. 63, 522-533
57. Stanisavljević A, Perić I, Gass P, Inta D, Lang UE, Borgwardt S, Filipović D (2019): Brain sub/region-specific effects of olanzapine on c-Fos expression of chronically socially isolated rats. Neuroscience 396, 46-65
58. Sun Y, Oberley LW, Li Y (1988): A simple method for clinical assay of superoxide dismutase. Clin. Chem. 34, 497-500
59. Temel Y, Kucukler S, Yıldırım S, Caglayan C, Kandemir FM (2020): Protective effect of chrysin on cyclophosphamide-induced hepatotoxicity and nephrotoxicity via the inhibition of oxidative stress, inflammation, and apoptosis. Naunyn-Schmiedeberg's Archives of Pharmacology 393, 325-337
60. Virag L (2005): Structure and function of poly (ADP-ribose) polymerase-1: role in oxidative stress-related pathologies. Curr. Vasc. Pharmacol. 3, 209-214
61. Wu A, Ren T, Hu Q, Liu Y (2000): Deltamethrin induces altered expression of P53, Bax and Bcl-2 in rat brain. Neurosci. Lett. 284, 29-32
62. Yousef MI, Awad TI, Mohamed EH (2006): Deltamethrin-induced oxidative damage and biochemical alterations in rat and its attenuation by Vitamin E. Toxicology 227, 240-247

63. Yu H-m, Wu Y, Ju P, Wang B-h, Yang X-d, Wang H-m, Xu L-c (2014): eNOS-JNK1-AR signaling pathway mediates deltamethrin-induced germ cells apoptosis in testes of adult rats. Environ. Toxicol. Pharmacol. 38, 733-741

Figures

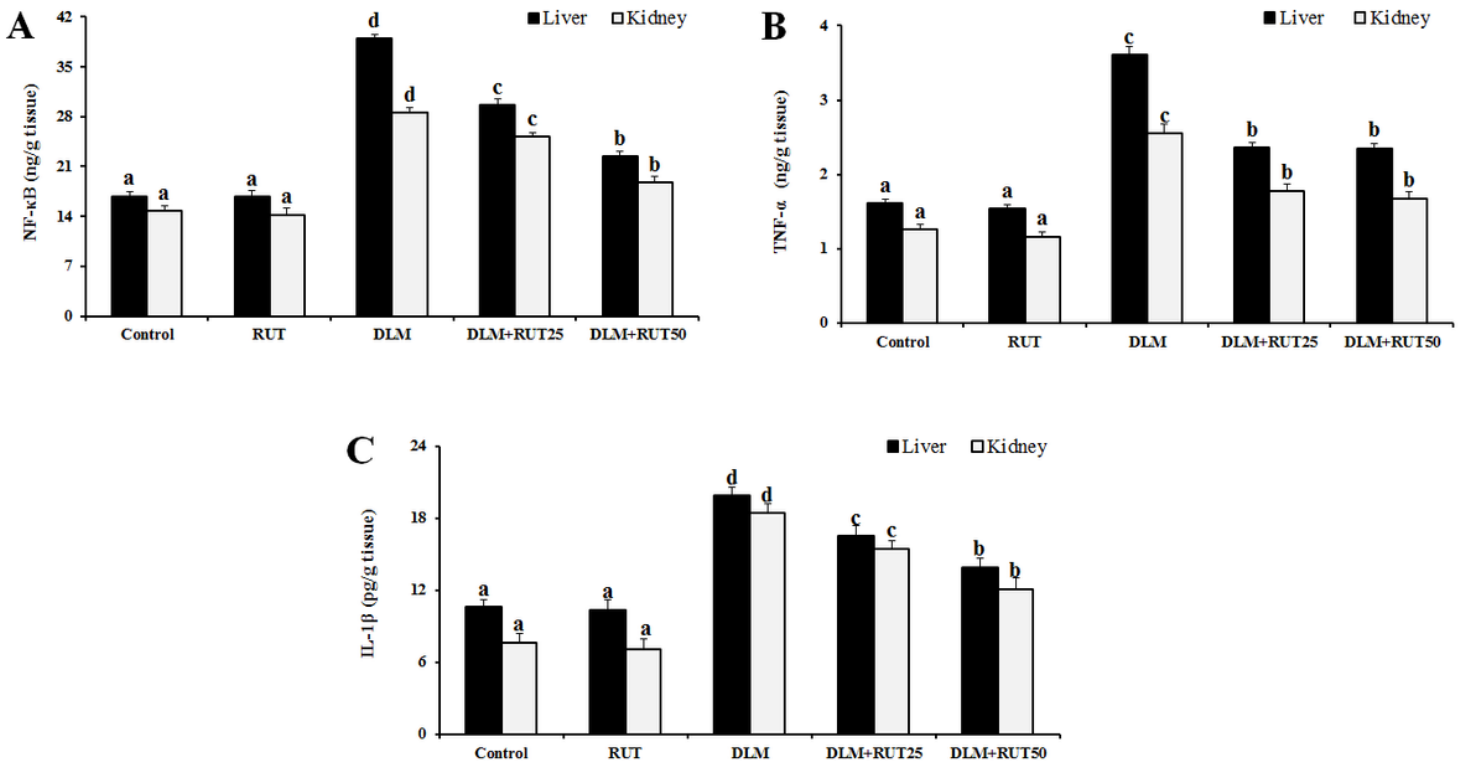

Figure 1

(A) Effect of RUT on DLM-induced liver and kidney NF-κB levels. (B) Effect of RUT on DLM-induced liver and kidney TNF-α levels. (C) Effect of RUT on DLM-induced liver and kidney IL-1β levels. Values are expressed as mean ± SEM. Different letters (a–d) on the columns show a statistical difference ($p < 0.05$).

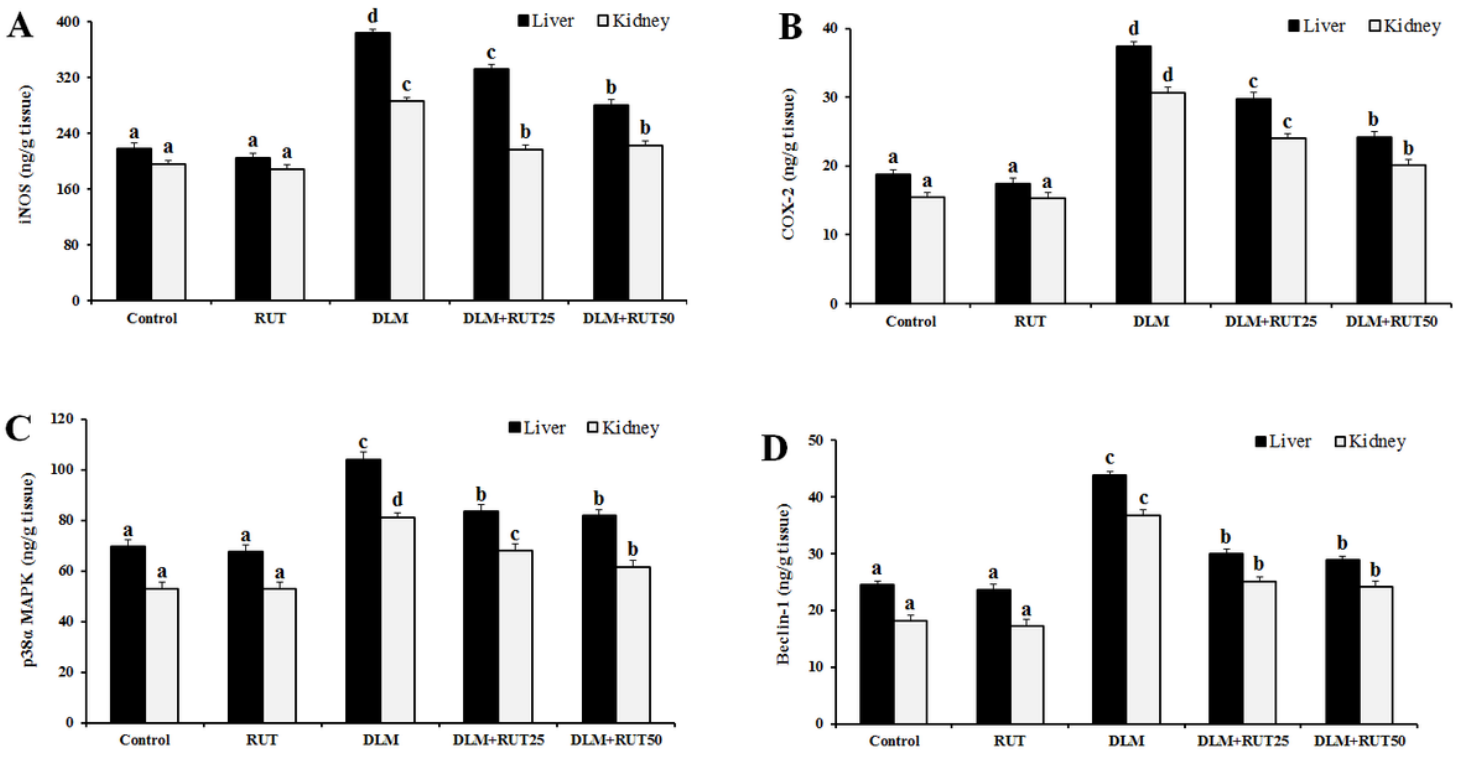

Figure 2

(A) Effect of RUT on DLM-induced liver and kidney iNOS activities. (B) Effect of RUT on DLM-induced liver and kidney COX-2 activities. (C) Effect of RUT on DLM-induced liver and kidney p38α MAPK activities. (D) Effect of RUT on DLM-induced liver and kidney beclin-1 levels. Values are expressed as mean ± SEM. Different letters (a–d) on the columns show a statistical difference ($p < 0.05$).

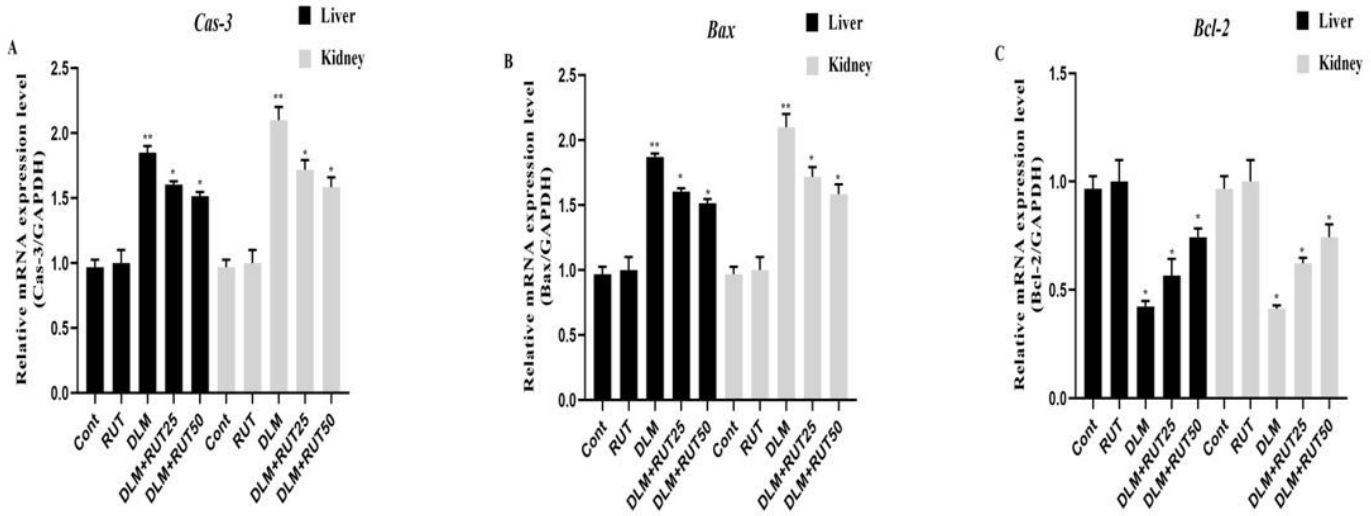

Figure 3

The mRNA transcript level of Cas-3, Bax, and Bcl-2 in the liver and kidney tissues of rat. Values represent the mean ± SEM of 3 indipendent samples; error bars indicate standard deviation. Statistical significance (* p 0.05, ** p<0.01, *** p<0.001) was analyzed using One Way ANOVA. A) Represent the relative mRNA expression levels of Cas-3. B) Represent the relative mRNA expression levels of Bax. C) Represent the relative mRNA expression levels of Bcl-2.

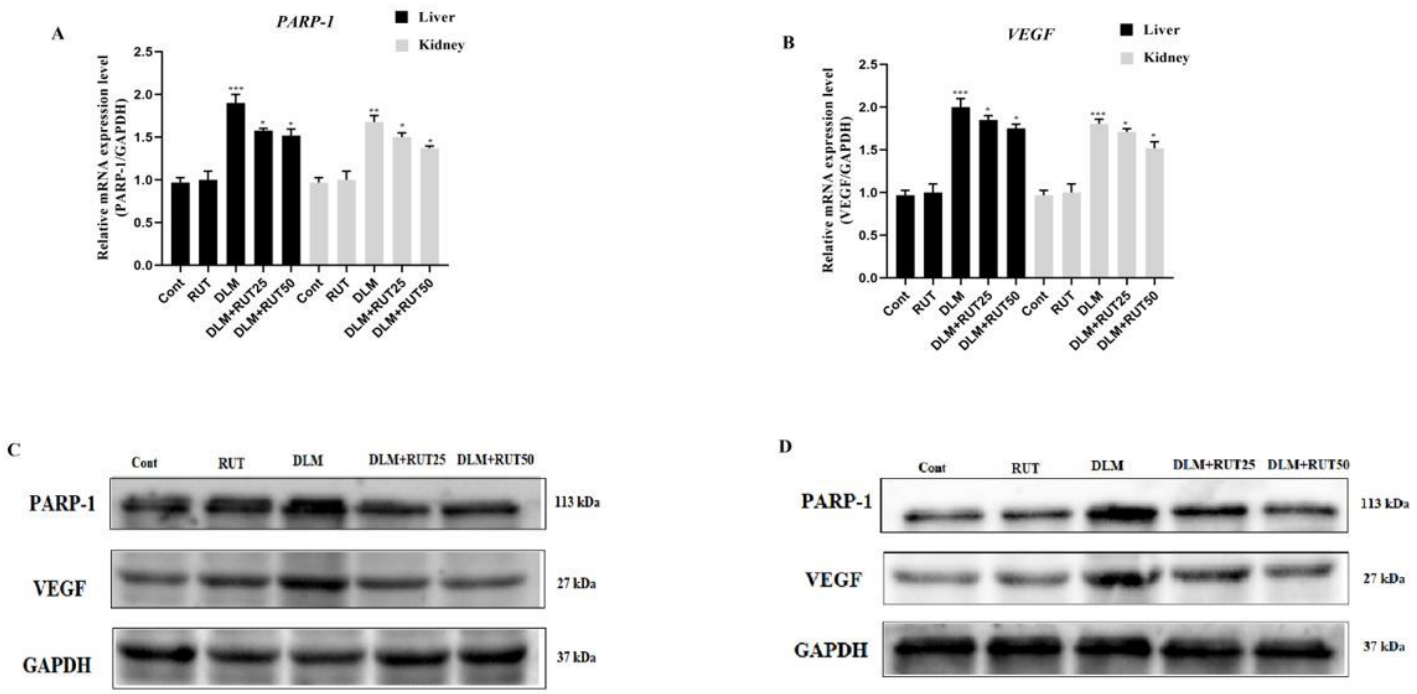

Figure 4

RT-PCR and Western blot results of PARP-1 and VEGF in liver and kidney tissues. A) Represent the relative mRNA expression levels of PARP-1. B) Represent the relative mRNA expression levels of VEGF. C) Equal quantities of total PARP-1, VEGF, and GAPDH protein from different samples (from left to right: control, RUT, DLM, DLM+RUT25, and DLM+RUT50). Total protein was extracted from the liver tissues of rat. D) Equal quantities of total PARP-1, VEGF, and GAPDH protein from different samples (from left to right: control, RUT, DLM, DLM+RUT25, and DLM+RUT50). Total protein was extracted from the kidney tissues of rat.

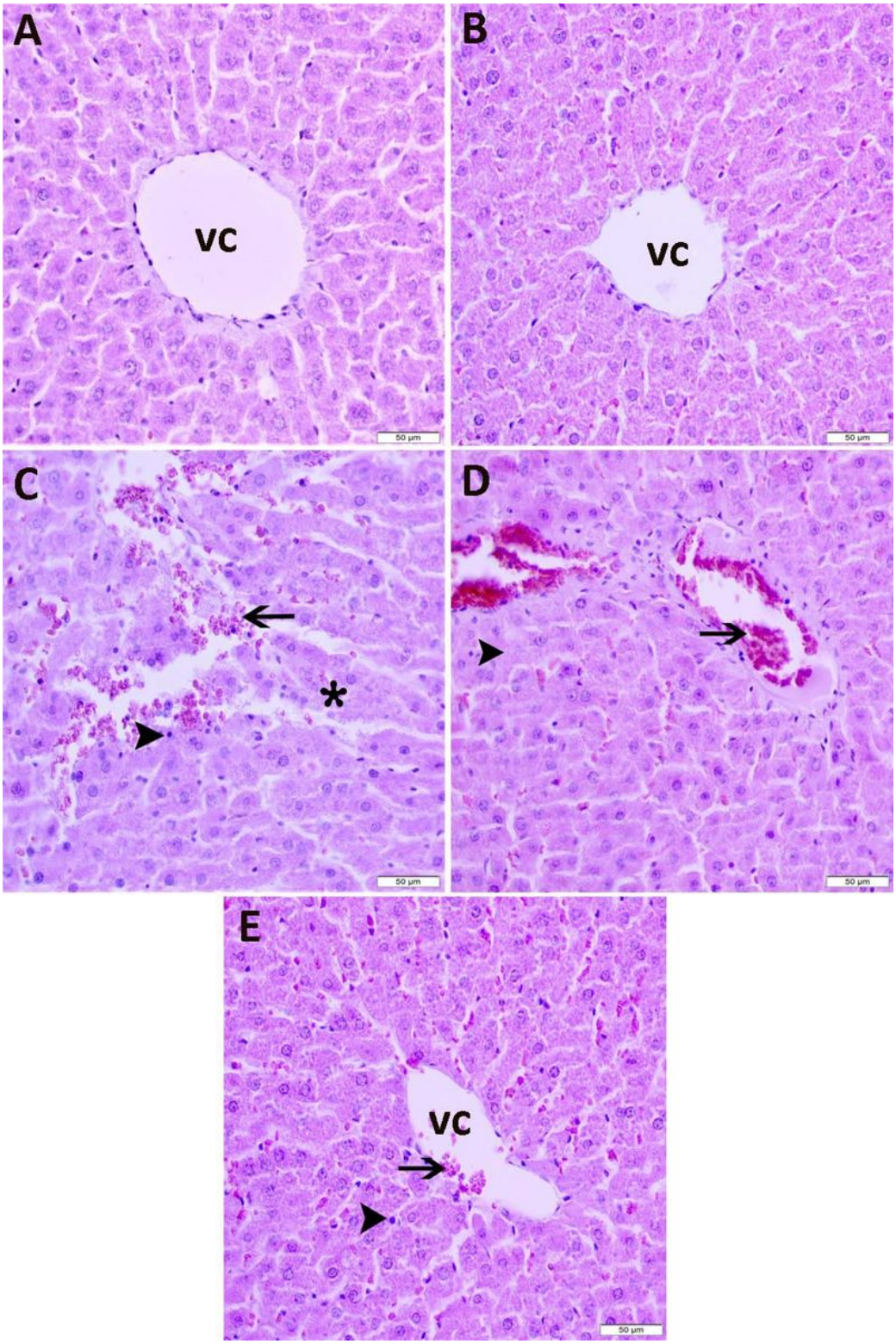

Figure 5

Microscopic view of the liver section obtained from control, RUT, DLM, DLM+RUT 25, and DLM+RUT50 treated rats. A) and B) Normal liver histology was shown in control and RUT-treated groups. C) Severe hemorrhage (arrow), nuclear pyknosis (arrowhead), and dissociation in hepatocytes (asterisk) were shown in DLM-treated group. D) In the DLM+RUT25 group, liver tissue seemingly severe congestion

(arrow) and moderate necrosis (arrowhead) rather than to severe hemorrhage. E) Mild congestion (arrow) and nuclear pyknosis (arrowhead) were shown in DLM+RUT50 group. (H&E stain, 400×)

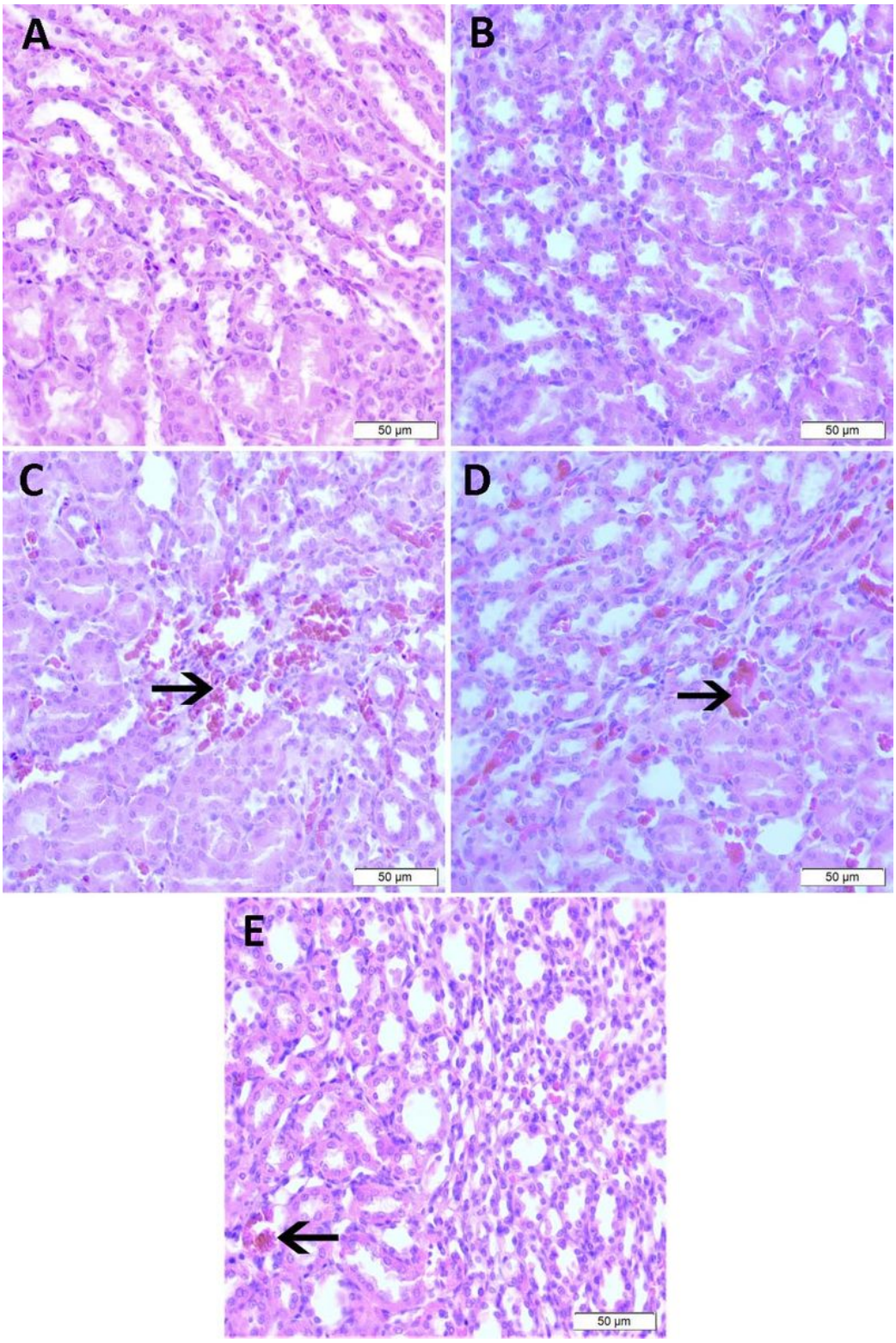

Figure 6

Microscopic view of the kidney section obtained from control, RUT, DLM, DLM+RUT 25, and DLM+RUT50 treated rats. A) and B) Normal kidney histology was shown in corticomedullary juntion of control and RUT-treated groups C) Severe hemorrhage (arrow) were shown in DLM-treated group. D) A mild reduction

of the hemorrhage (arrow) were shown in DLM+RUT25 group. E) Mild hemorrhage (arrow) were shown in DLM+RUT50 group. (H&E stain, 400×)

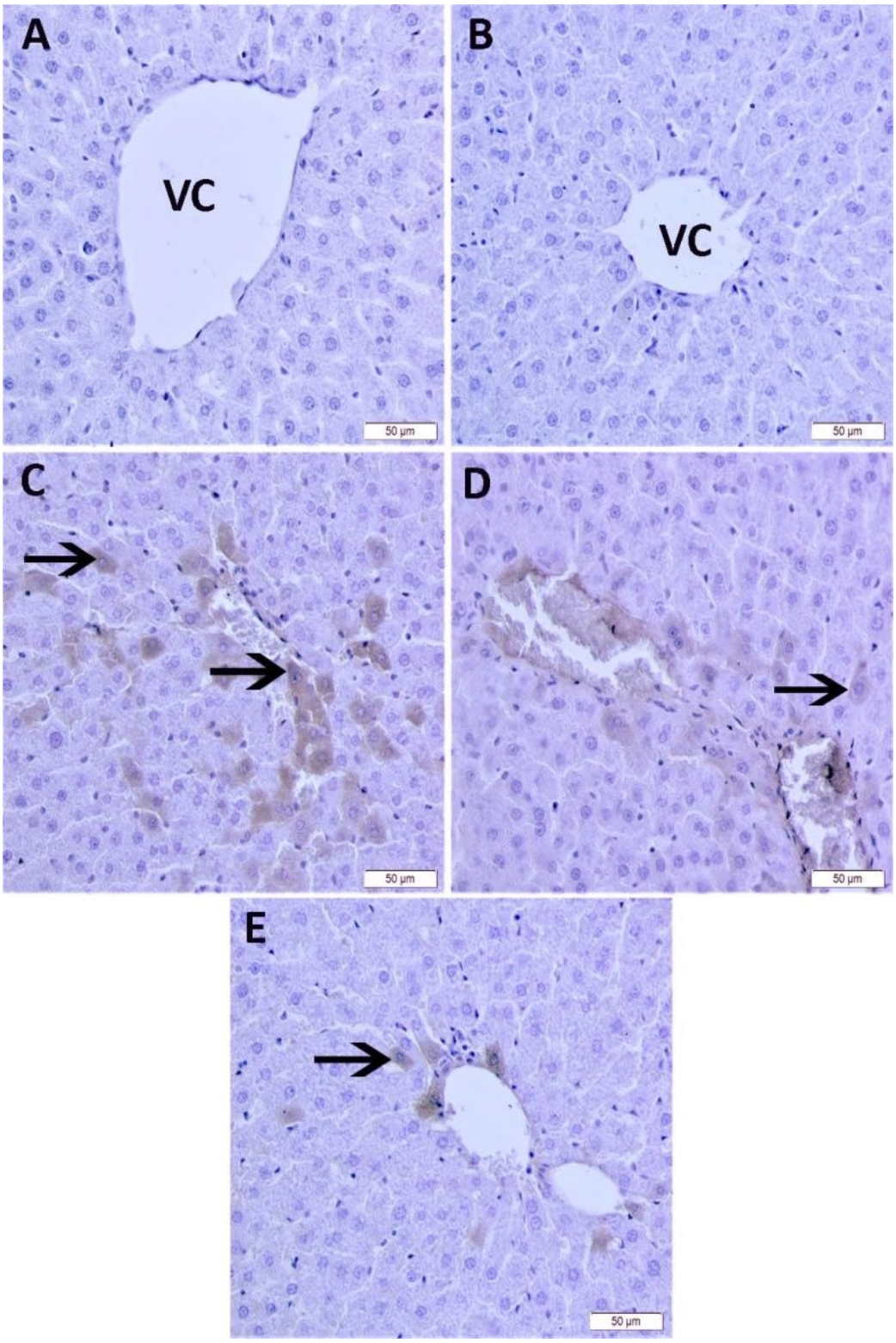

Figure 7

Effect of RUT on immunohistochemical stain of c-fos in livers of DLM-treated rats. A) Control group; B) RUT-treated group; C: DLM-treated group; D) DLM+RUT25 group, and E) DLM+RUT50 group.

Immunostaining was performed using a specific antibody against c-fos. The positive staining of c-fos is presented as brown hepatocytes (arrows), (vc, central vein). (IHC stain, 400×).

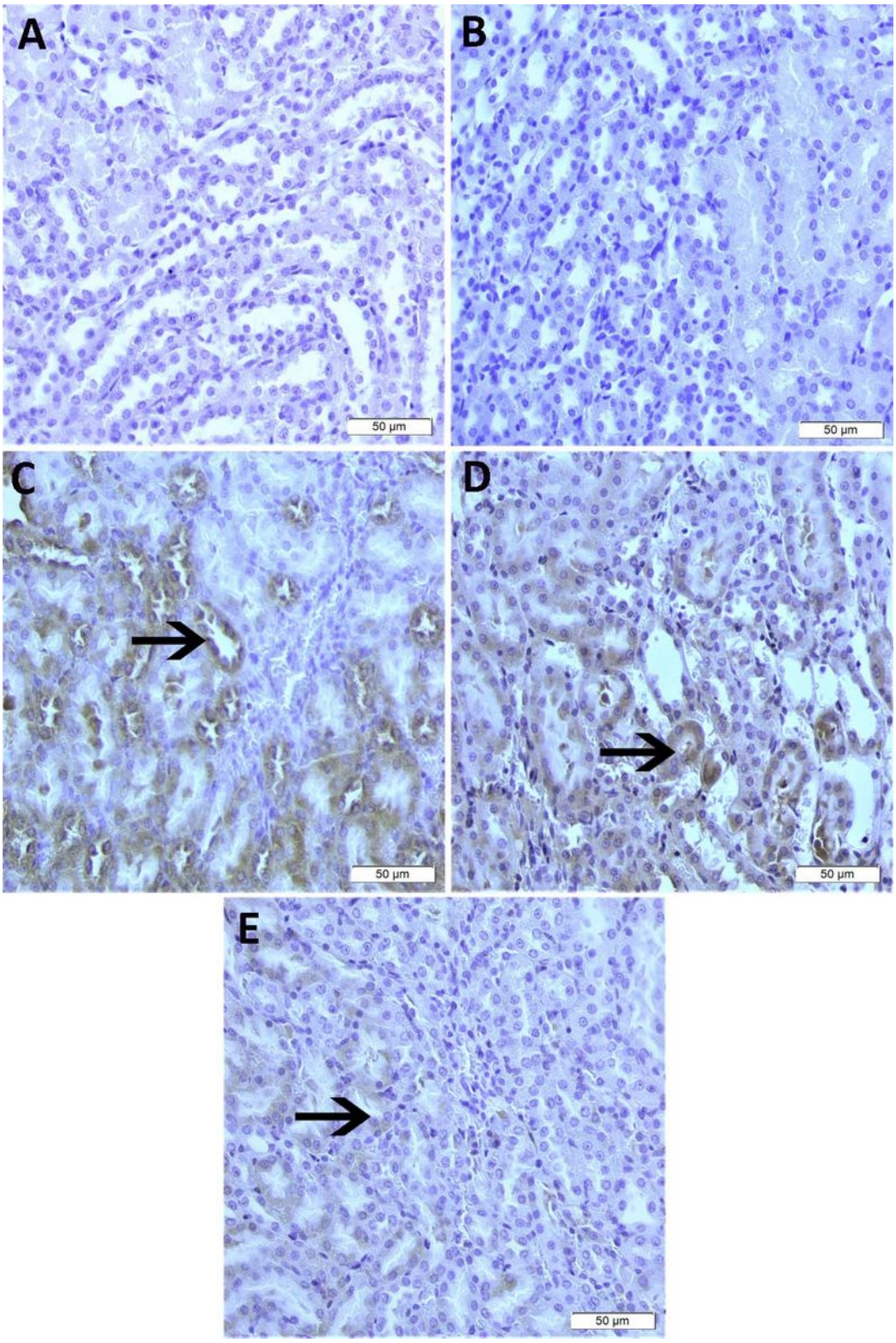

Figure 8

Effect of RUT on immunohistochemical stain of c-fos in kidneys of DLM-treated rats. A) Control group, B) RUT-treated group; C) DLM-treated group, D) DLM+RUT25 group, and E) DLM+RUT50 group. The positive staining of c-fos is presented as brown corticomedullary tubules (arrows), (IHC stain, 400×).

Supplementary Files

This is a list of supplementary files associated with this preprint. Click to download.

- Dlmandrutingraphicalabstract.docx